

Electrons and phonons at sub-Kelvin temperatures: validation of the disorder-mediated scattering theory

I. J. Maasilta, J. T. Karvonen, J. M. Kivioja*, and L. J. Taskinen

NanoScience Center, Department of Physics, P.O. Box 35, FIN-40014 University of Jyväskylä, Finland

(Dated: January 28, 2020)

We have used symmetric normal metal-insulator-superconductor (NIS) tunnel junction pairs, known as SINIS structures, for ultrasensitive thermometry in the temperature range 50 - 700 mK. By Joule heating the electron gas and measuring both the electron and the lattice temperatures simultaneously, we show for the first time that the electron-phonon (e-p) scattering rate in a well studied and common disordered thin-film material (Cu) follows a T^4 temperature dependence. This power law is indicative e-p coupling mediated by vibrating disorder, in contrast to the previously observed T^3 and T^2 laws.

Although the interaction between conduction electrons and thermal phonons is elementary for many processes and phenomena at low temperatures, there are still relatively few experimental studies that conclusively support the theoretical description, particularly for typical disordered thin film samples. Several earlier results [1, 2, 3] indicated that even for disordered films, the temperature dependence for the electron-phonon (e-p) scattering rate $1/\tau_{e-p}$ follows the power law expected for pure samples with coupling to longitudinal phonons only: $1/\tau_{e-p} \sim T^3$ [4]. These results confirmed the relation $P = \Sigma\Omega(T_e^5 - T_p^5)$ between heating power P and electron and phonon temperatures T_e and T_p in a volume Ω , and it is widely used for thin film metallic samples at low temperatures (Σ is a material dependent parameter). However, the theory for disordered thin films [5, 6, 7, 8] predicts that the scattering rate from vibrating disorder (impurities, boundaries) is $1/\tau_{e-p} \sim T^4$ in the limit $ql < 1$, where q is the wavevector of the dominant thermal phonons and l the electron mean free path. This leads to the relation

$$P = \Sigma'\Omega(T_e^6 - T_p^6), \quad (1)$$

a result that has not been widely confirmed. In fact, we are not aware of any observation of it in standard normal metal films like Cu, Al, Au etc., and only suggestive evidence exists for strongly disordered ($l \sim 1$ nm) Ti, Hf [9] and Bi [10] films.

Here, we report the first observation of disorder-mediated electron-phonon (e-p) scattering in ordinary, evaporated Cu thin films. We have measured the rate at which electrons in a normal metal (Cu) wire overheat, when DC power is applied to it by Joule heating. This technique has been shown [1, 2, 3] to give the energy-loss rate directly, in contrast to the temperature dependence of the weak localization resistance [11], which gives the dephasing rate [12]. The overheating rate is determined directly by measuring the electron temperature with the help of symmetric normal metal-insulator-superconductor (NIS) tunnel junction pairs, known as SINIS structures. SINIS-thermometers have been shown

[13, 14, 15] to be extremely sensitive thermometers, operating at the lowest experimentally achievable temperatures. Therefore, they are also candidates for ultrasensitive microbolometers [16, 17] in the sub-Kelvin temperature range.

Samples used in this work have two Cu normal metal wires of length ~ 500 μm , and width ~ 300 nm, separated by a distance 2 μm and electrically isolated from each other, as shown in the SEM image [Fig. 1(a)]. They were fabricated by e-beam lithography and three-angle shadow-mask evaporation technique on thermally oxidized (oxide thickness 250 nm) Si substrates, with four film thicknesses t varying from 35 nm to 180 nm (Table I). The deposition was done by e-beam evaporation in a UHV chamber with a growth rate $\sim 2 - 3$ \AA/s . The normal metal wires were connected to the measurement circuit by superconducting Al leads. One pair of leads forms SINIS tunnel junctions for each wire, and are used to measure the electron temperature. These tunnel junctions were formed by thermal oxidation of the Al films in 50 mbar of O_2 for 5 min. In contrast, the junctions connecting the lower wire to a voltage source (Fig. 1) are NS-junctions without tunneling barriers, and are used to heat the sample. Clean NS-junctions have a small electrical resistance compared to the residual low-temperature resistance of the wire (between 100 and 1500 Ω for all the samples). Thus, for low enough heating voltages the NS-junctions are biased within the superconducting gap Δ of the leads, and the process of Andreev reflection can take place making the junctions good thermal insulators despite being electrically conducting. When this takes place, we can achieve conditions in which the wire is uniformly Joule heated [18]. In addition, the thermal resistance of the tunnel junctions is estimated to be at least an order of magnitude larger than the thermal resistance due to the e-p coupling, R_{e-p} , at the temperature range of this experiment [20], and can be neglected in the analysis.

To assess the quality of all the Cu films used, we measured their resistivities and used those results to calculate the electron mean free paths l , yielding values from 21 nm to 62 nm depending on film thickness (Table I).

Since l appears to be a significant fraction of the film thickness for both films, we surmise that boundary scattering is important in these samples. Using a transverse sound velocity $c_t = 2300$ m/s for Cu [21], we estimate the critical phonon temperatures T_p^{crit} , where $ql = 1$, shown in Table I. It is evident that these temperatures lie well within our experimental temperature range, so both regimes $ql < 1$ and $ql > 1$ are accessible.

All measurements were performed by current biasing the two SINIS thermometers and measuring their DC voltages simultaneously [Fig 1(b)] in a dilution refrigerator with a base temperature ≈ 60 mK. The thermometers were calibrated by varying the bath temperature (T_{bath}) of the refrigerator very slowly, to ensure the sample stage was in equilibrium with the bath. The temperature of the sample stage was measured with a calibrated Ruthenium Oxide thermometer. Figure 2 shows an example of such a calibration measurement for the lower wire in Fig. 1 for two different samples, one without filtering in the cryostat (s3) and one with RC-filters at 4.2 K (s1). All upper wire calibration curves resembled the s1 data in Fig 2 very closely even without filtering. The theoretical curves (red) were calculated numerically from the BCS theory. This calculation has essentially no free parameters, since the current bias I is known and R_T , and Δ are determined independently from the I-V characteristics (not shown). The agreement with the data is good except at the very lowest temperatures, where a deviation can be seen in both samples, more clearly so in sample s3. This deviation could arise by at least two major mechanisms: (i) a component of leakage or noise current affects the measurement, and (ii) the electrons overheat at the low- T range (thermometer electron temperature T_e is higher than the sample stage temperature T_{bath}). We have ruled out (i) by directly measuring the responsivities dV/dP of the thermometers as a function of I using a lock-in amplifier (Fig. 2 inset). The theoretical dV/dP is a monotonically decreasing function of I . However, experimentally, at low I the responsivity deviates from theory and we find a maximum. Thus, by setting $I \geq 200$ pA into the BCS-theory regime problem (i) can be avoided. Mechanism (ii), overheating by noise power P_{noise} is an obvious explanation since the filtering clearly improves the situation. It has been modeled with the help of the theory for e-p scattering and the Kapitza-resistance [22]: $P_{noise} = A(T_e^n - T_p^n) = B(T_p^4 - T_{bath}^4)$, where $n = 4, 5, 6$, $A = \Sigma' \Omega$ and $B = \sigma S$ are parameters of the sample, S being the area of the Kapitza-boundary. Eliminating T_p from these equations, we get a relation $T_{bath} = [(T_e^n - P_{noise}/A)^{4/n} - P_{noise}/B]^{1/4}$, with two free parameters, P_{noise}/A and P_{noise}/B .

Including the heating model, all calibration curves have essentially perfect fits to the model, and varying n did not affect on the goodness of fit. [examples shown in Fig. 2 (blue)]. Thus, the thermometers are calibrated

correctly by reading T_e from the BCS-theory curve, e.g. in Fig. 2, $V_{sinis} = 0.32$ mV for s3 corresponds to $T_e = 0.13$ K, *not* to 0.06 K. We do not have an independent estimate for P_{noise} in this measurement, thus extraction of Σ' or σ is not possible [23].

Using the calibrated SINIS thermometers, we then studied what happened when only the lower wire is directly heated by Ohmic dissipation at $T_{bath} = 60$ mK. Heating power was applied by slowly ramping a DC voltage across the wire connected by the NS-junctions. The power P was determined by measuring the heating current and voltage across the wire directly in a 4-wire configuration. It should be noted that the SINIS circuit is fully floating with respect to the heating circuit, thus no heating current flows through the SIN junctions. In Fig 3 we plot the electron temperatures in both wires vs. P obtained from several sweeps for all samples. As can be seen, *both* temperatures rise when heating power is increased. This means that the upper wire is heated indirectly by phonons, since there is no direct electrical contact. Since these phonons can only strike the film from below, there must be a mechanism in the substrate to backscatter hot phonons generated in the lower wire (corresponding to a distribution different from the thermal distribution at T_{bath}). Most likely, this scattering takes place in the oxide layer and/or at the interface between the oxide and the silicon substrate [24]. Also, bulk scattering of long wavelength phonons in the crystalline Si lattice is negligible [25]. Clearly, above a few pW this phonon heating dominates the signal over the noise heating in the upper wire (Fig 3). Thus, we can identify its temperature as the *phonon* temperature T_p , since all the power absorbed from the phonons has to be re-emitted back into the substrate (no net heat flow). Moreover, since the two wires are separated only by $\sim 2\mu\text{m}$, much longer than the lateral mean free path of phonons in SiO [22], the same T_p is seen by the lower wire also. The conclusion is that we can simultaneously measure the electron and phonon temperatures of the lower wire while it is being overheated. Boundary resistance between the Cu film and the substrate is not important, since the relevant phonon wavelengths are much longer than the Cu film thickness for all samples.

Looking back at Fig. 3(a), we see that T_e for sample s1 scales as $(P/A)^{1/6}$ for approximately four orders of magnitude until $P \sim 600$ pW, where a crossover to $(P/A)^{1/5}$ takes place. In Fig. 3(b), samples s2 and s3 also behave in a similar manner, where T_e changes from $(P/A)^{1/n}$, $n > 5$, to $(P/A)^{1/5}$ at $P \sim 300$ pW for s2 and at $P \sim 50$ pW for s3 [26]. For s2 and s3, these crossover points correspond surprisingly well to the independently determined values of T_p^{crit} (Table I). However, for s1 the experimental transition is a factor three lower. Since $T_e^n \gg T_p^n$ for samples s1-s3, Fig. 3 gives significant evidence for the validity of Eq. (1) when $ql < 1$ and for a crossover to the common T^5 law when $ql > 1$. Sample

s4 appears inconsistent, with a non-integer $n = 4.6$ for $ql > 1$. However, it is clear that for s4 the log-log plot is not the correct way to analyze the data, because the condition $T_e^n \gg T_p^n$ is not satisfied as it is for the other samples.

To obtain a more complete picture with accurate analysis for all samples, Fig. 4 presents the data from the same runs in linear scale, with the power n in the expression $T_e^n - T_p^n$ varied from 4 to 6. For samples s1-s3 we have plotted only data for $ql < 1$, whereas for s4 only data at $ql > 1$ is shown. It is very clear that $n = 4$ does not fit the data [Fig. 4(a),(d)], showing that we are not dominated by the Kapitza resistance, or by e-p scattering mediated by static disorder [8]. Also, the expected theory for pure samples, $n = 5$ [Fig. 4(b),(e)], only fits sample s4, as the one-parameter linear fits through the origin do not fit the data for the other samples. In contrast, $n = 6$ [Fig. 4(c),(f)] gives consistent results for s1, s2 and s3. From the linear fits through the origin we get $\Sigma' = 1 - 2 \times 10^{10} \text{ W/K}^6 \text{m}^3$ for s1-s3 and $\Sigma = 7 \times 10^9 \text{ W/K}^5 \text{m}^3$ for s4. Comparing Σ' with the microscopic theory gives a reasonable result $c_t = 1800 - 2300 \text{ m/s}$.

In conclusion, we have for the first time obtained clear evidence that the electron-phonon scattering rate scales with temperature as $1/\tau_{e-p} \sim T^4$ in disordered, evaporated Cu thin films. This power law corresponds to electrons scattering from transverse phonons mediated by boundaries, impurities, vacancies etc. that are vibrating together with the phonon mode. In contrast, e-p scattering in the presence of static disorder leads to $1/\tau_{e-p} \sim T^2$, a result that has been confirmed in many materials and samples [11]. Our result has several practical consequences. Compared to a lower power dependence, it is harder to cool the electrons with cold phonons, i.e. the electron gas decouples from the lattice more strongly at the lowest temperatures. Direct electron cooling [14, 15] then becomes more important. On the other hand, this means that a sensor based on hot electron effects is even more sensitive, since the ultimate noise equivalent power of such a detector is proportional to $1/R_{e-p}^{1/2}$. We stress that in order to obtain $1/\tau_{e-p} \sim T^4$ the sample needs to be a regular metal, have $ql < 1$, contain little non-vibrating disorder and have 3D phonons coupled to electrons by the deformation potential. We believe most earlier experiments do not satisfy all these conditions (e.g. Ref. [1] has $ql > 1$, Ref. [27] has a suspended GaAs substrate, Refs. [2, 3, 28] studied alloys and Ref. [29] studied degenerately doped Si in the strong screening limit.)

We thank D.-V. Anghel, M. P. Bruijn, A. N. Cleland, J. P. Pekola, H. Pothier, A. Savin and A. Sergeev for discussions. This work was supported by the Academy of Finland under the Finnish Center of Excellence Program 2000-2005 (Project No. 44875, Nuclear and Condensed Matter Physics Program at JYFL).

[*] Present Address: Low Temperature Laboratory, P. O. Box 2200, FIN-02015 HUT, Finland

[1] M. L. Roukes, M. R. Freeman, R. S. Germain, R. C. Richardson, and M. B. Ketchen, Phys. Rev. Lett. **55**, 422 (1985).

[2] M. Kanskar and M. N. Wybourne, Phys. Rev. Lett. **73**, 2123 (1994).

[3] F. C. Wellstood, C. Urbina, and J. Clarke, Phys. Rev. B **49**, 5942 (1994).

[4] V. F. Gantmakher, Rep. Prog. Phys. **37**, 317 (1974).

[5] A. Schmid, Z. Phys. **259**, 421 (1973); in *Localization, Interaction and Transport Phenomena*, Springer 1985.

[6] B. L. Altshuler, Zh. Eksp. Teor. Fiz. **75**, 1330 (1978) [Sov. Phys. JETP **48**, 670 (1986)].

[7] M. Yu. Reizer and A. V. Sergeev, Zh. Eksp. Teor. Fiz. **90**, 1056 (1986) [Sov. Phys. JETP **63**, 616 (1986)].

[8] A. Sergeev and V. Mitin, Phys. Rev. B **61**, 6041 (2000); Europhys. Lett. **51**, 641 (2000).

[9] M. E. Gershenson, D. Dong, T. Sato, B. S. Karasik, and A. V. Sergeev, Appl. Phys. Lett. **79**, 2049 (2001).

[10] Yu. F. Komnik, V. Yu. Kashirin, B. I. Belevtsev, and E. Yu. Beliaev, Phys. Rev. B **50**, 15 298 (1994).

[11] For a recent review of the weak localization data, see J. J. Lin and J. P. Bird, J. Phys. Condens. Matter **14**, R501 (2002).

[12] The dephasing rate can equal the energy loss rate if the electron-phonon interaction is the only dephasing mechanism present. In general, one can imagine many other dephasing channels that do not influence the energy loss rate, a prime example being the electron-electron interaction, which by definition cannot lower the energy of the electron gas as a whole.

[13] J. M. Rowell and D. C. Tsui, Phys. Rev. B **14**, 2456 (1976).

[14] M. Nahum, T. M. Eiles, and J. M. Martinis, Appl. Phys. Lett. **65**, 3123 (1994).

[15] M. M. Leivo, J. P. Pekola, and D. V. Averin, Appl. Phys. Lett. **68**, 1996 (1996).

[16] M. Nahum and J. Martinis, Appl. Phys. Lett. **63**, 3075 (1993).

[17] L. Kuzmin, D. Chouvaev, M. Tarasov, P. Sundquist, M. Willander and T. Claeson, IEEE Trans. Appl. Supercond. **9**, 3186 (1999).

[18] For much shorter but otherwise equivalent wires, the NS junctions are quickly biased above the gap, and the heat leak through them has to be taken into account in the analysis [19].

[19] J. M. Kivioja, I. J. Maasilta, J. P. Pekola, and J. T. Karvonen, Physica E **18**, 21 (2003).

[20] D. V. Anghel and J. P. Pekola, J. Low Temp. Phys. **123**, 197 (2001).

[21] In the disordered limit, transverse phonon scattering is expected to be dominant over longitudinal phonons [8].

[22] E. T. Swartz and R. O. Pohl, Rev. Mod. Phys. **61**, 605 (1989).

[23] However, using the Σ' extracted from Fig. 4 for sample s3 for example, consistency is achieved with $P_{noise} = 0.1 \text{ pW}$, a reasonable value.

[24] Since the contact area between the substrate and the sample stage is macroscopically large, the Kapitza resistance associated with it is small. We also attached the

substrate to the sample stage by two different ways, with GE-7031 varnish and with silver paint, without any difference in results.

[25] J. A. Shields, S. Tamura and J. P. Wolfe, Phys. Rev. B **43**, 4966 (1991).

[26] Due to the larger noise heating in samples s2 and s3 it is too difficult to say with certainty whether $n = 6$ below $ql = 1$ based on Fig. 3(b) alone.

[27] C. S. Yung, D. R. Schmidt, and A. N. Cleland, Appl. Phys. Lett. **81**, 31 (2002).

[28] J. F. DiTusa, K. Lin, M. Park, M. S. Isaacson, and J. M. Parpia, Phys. Rev. Lett. **68**, 1156 (1992).

[29] P. Kivinen, A. Savin, M. Zgirski, P. Törmä, J. Pekola, M. Prunnila, and J. Ahopelto, J. Appl. Phys. **94**, 3201

(2003).

TABLE I: Parameters of Cu films studied. $T_p^{crit} = \hbar c_t / (2.82kl)$, where we used $c_t = 2300$ m/s.

sample	t (nm)	RRR	$\rho_{4.2K}$ ($\mu\Omega\text{cm}$)	l (nm)	T_p^{crit} (K)
s1	35	1.8	3.06	21.4	0.29
s2	45	2.1	2.26	29.0	0.22
s3	90	2.5	1.32	49.7	0.13
s4	180	3.2	1.06	61.9	0.10

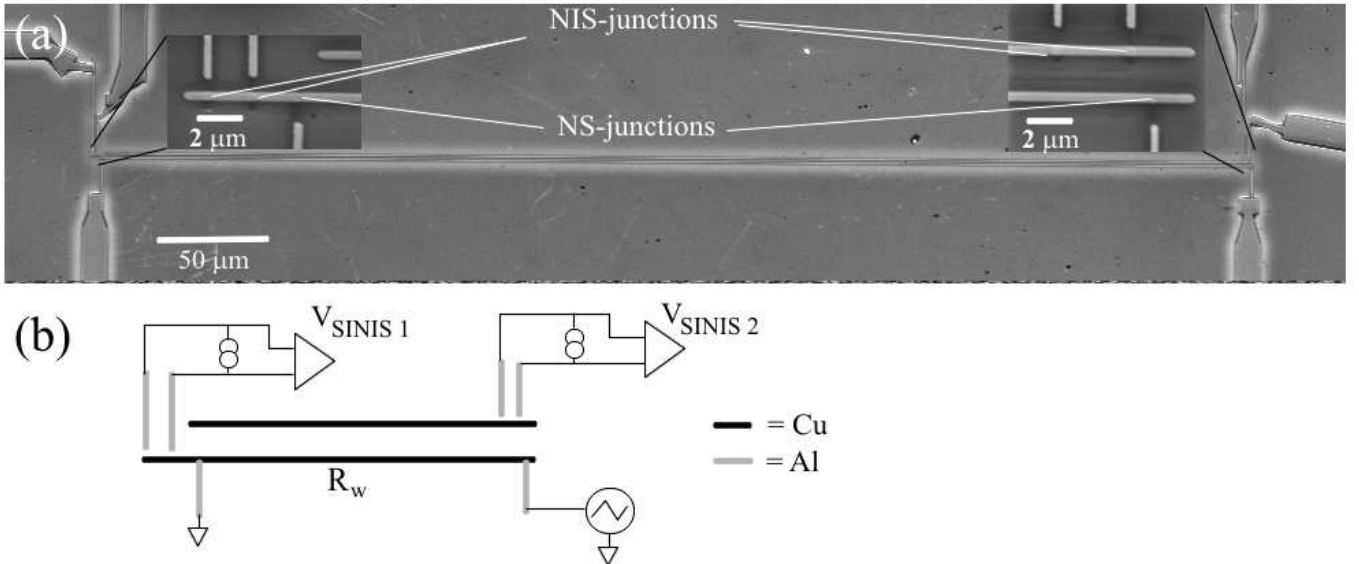


FIG. 1: (a) An SEM image of a sample. The horizontal lines are Cu wires, the vertical lines are Al leads that form the junctions at the intersections with the Cu line. The insets are enlargements of the areas where the junctions are located. Note that the pure Al vertical lines (black) make contact with the horizontal Cu lines, the lighter gray vertical lines consist of Al+shadows from the Cu evaporation. (b) A schematic of the sample and the measurement circuit.

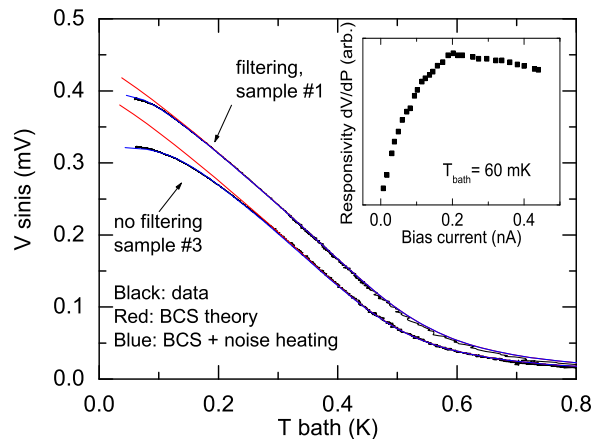


FIG. 2: (color) Calibration data for the SINIS junctions connected to the lower wire in Fig. 1 (samples s1 and s3), biased at $I = 200$ pA. Black lines are the experimental data, red lines the BCS-theory result, and blue lines the BCS-theory and a noise heating model, as explained in the text. Δ and R_T were determined independently from the I-V characteristics. To obtain agreement with the calibration data Δ needed to be adjusted by $\sim 10\%$ for s3 and by $\sim 5\%$ for s1 compared to the I-V value. From this data we estimate the temperature sensitivity $\delta T = (dT/dV)\delta V \approx 0.1$ mK rms, where δV is the rms noise voltage. Inset: Measured responsivity dV/dP of a SINIS vs. the bias current.

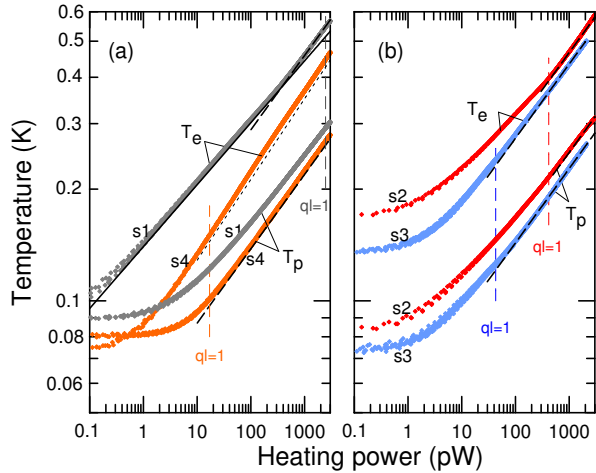


FIG. 3: (color) (a) The electron (lower wire in Fig 1) and phonon (upper wire in Fig.1) temperatures of samples s1 (grey) and s4 (orange) vs. applied Joule heating power in log-log scale. Solid line is a guide to the eye of the form $T = (P/A)^{1/6}$, corresponding to the disordered e-p scattering theory [Eq. (1)]. Dashed lines have $T = (P/A)^{1/5}$, the dotted line $T = (P/A)^{1/4.6}$. Vertical lines mark the values of P where $ql = 1$. The NS leads were filtered for s1 and s4. (b) Same for samples s2 (red) and s3 (blue), the NS leads were not filtered. $T_{bath} = 60$ mK.

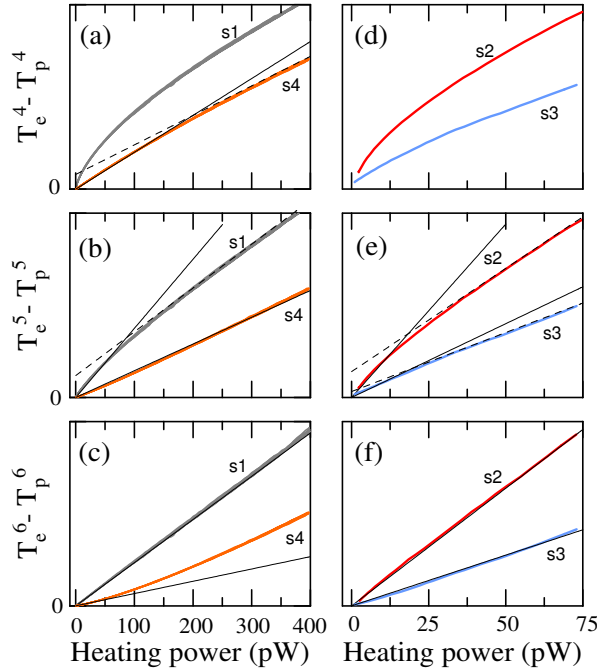


FIG. 4: (color) $T_e^n - T_p^n$ (arbitrary scale) vs. Joule heating power [including a small noise power contribution for samples s2 and s3 ~ 1 pW, calculated from Fig. 3(b)], with (a) $n = 4$, (b) $n = 5$, (c) $n = 6$ for samples s1 and s4, and (d) $n = 4$, (e) $n = 5$, (f) $n = 6$ for samples s2 and s3. The origin for the s4 data has been shifted to the point corresponding to $ql = 1$ to highlight the $ql > 1$ regime. Solid lines are one parameter fits through the origin, dashed lines two parameter linear fits (theoretically unjustified). $T_{bath} = 60$ mK.